tvst

Article

Using the Lens Paradox to Optimize an In Vivo MRI-Based Optical Model of the Aging Human Crystalline Lens

Alyssa L. Lie[1], Xingzheng Pan[1], Thomas W. White[2], Paul J. Donaldson[3], and Ehsan Vaghefi[1]

[1] School of Optometry and Vision Science, New Zealand National Eye Centre, University of Auckland, Auckland, New Zealand
[2] Department of Physiology and Biophysics, Stony Brook University, Stony Brook, NY, USA
[3] Department of Physiology, School of Medical Sciences, New Zealand National Eye Centre, University of Auckland, Auckland, New Zealand

Correspondence: Ehsan Vaghefi, School of Optometry and Vision Science, New Zealand National Eye Centre, University of Auckland, Auckland 1010, New Zealand. e-mail: e.vaghefi@auckland.ac.nz

Received: June 3, 2020
Accepted: June 23, 2020
Published: July 28, 2020

Keywords: Magnetic resonance imaging; lens paradox; crystalline lens; lens physiological optics; optical modeling; clinical observational study; gradient of refractive index; in vivo

Citation: Lie AL, Pan X, White TW, Donaldson PJ, Vaghefi E. Using the lens paradox to optimize an in vivo MRI-based optical model of the aging human crystalline lens. Trans Vis Sci Tech. 2020;9(8):39, https://doi.org/10.1167/tvst.9.8.39

Purpose: To optimize our in vivo magnetic resonance imaging (MRI)-based optical model of the human crystalline lens, developed with a small group of young adults, for a larger cohort spanning a wider age range.

Methods: Subjective refraction and ocular biometry were measured in 57 healthy adults ages 18 to 86 years who were then scanned using 3T clinical magnetic resonance imaging (MRI) to obtain lens gradient of refractive index (GRIN) and geometry measurements. These parameters were combined with ocular biometric measurements to construct individualized Zemax eye models from which ocular refractive errors and lens powers were determined. Models were optimized by adding an age-dependent factor to the transverse relaxation time (T_2)-refractive index (n) calibration to match model-calculated refractive errors with subjective refractions.

Results: In our subject cohort, subjective refraction shifted toward hyperopia by 0.029 diopter/year as the lens grew larger and developed flatter GRINs with advancing age. Without model optimization, lens powers did not reproduce this clinically observed decrease, the so-called lens paradox, instead increasing by 0.055 diopter/year. However, modifying the T_2-n calibration by including an age-dependent factor reproduced the decrease in lens power associated with the lens paradox.

Conclusions: After accounting for age-related changes in lens physiology in the T_2-n calibration, our model was capable of accurately measuring in vivo lens power across a wide age range. This study highlights the need for a better understanding of how age-dependent changes to the GRIN impact the refractive properties of the lens.

Translational Relevance: MRI is applied clinically to calculate the effect of age-related refractive index changes in the lens paradox.

Introduction

Coined by Nicholas Brown in the 1970s, the term "lens paradox" describes the discrepancy in the relationship between crystalline lens shape and refractive power: The steepening of lens curvatures with age is not accompanied by an increase in lens power.[1,2] Unlike other ocular refractive structures, the lens grows throughout adulthood, getting thicker and rounder with age.[3–5] This change in lens geometry should therefore make the lens more powerful and increase its relative contribution to the refractive power of the eye. However, aging of the eye in adulthood has, in general, been associated with a hyperopic rather than myopic shift.[6–12] Due to the age independence of corneal power,[13–16] vitreous chamber depth,[5,13] and axial length,[13,14] the only variables left in the visual system are associated with the lens. The lens paradox has therefore been attributed mainly to age-dependent changes in the structure of the internal gradient refractive index (GRIN) of the lens.

Theoretical modeling has shown that the lens paradox can be explained by either an age-dependent reduction in refractive index variation across the GRIN[17,18] or a flattening of the GRIN profile.[17–20]

Table 1. Descriptive Characteristics of the Study Groups

Characteristic	Young (18–40 y)	Middle-Aged (41–60 y)	Older (>60 y)
Number	22	20	15
Age (y), mean ± SD	24 ± 4	51 ± 5	75 ± 7
Male, *n* (%)	10 (45)	12 (60)	6 (40)
Refraction (D), mean ± SD	−1.52 ± 1.70	−1.10 ± 1.83	0.40 ± 2.00

Studies investigating human lens GRIN using techniques ranging from ray tracing[21] to magnetic resonance imaging (MRI)[22–28] have consistently observed a gradual flattening of the GRIN profile with age to form a central plateau of constant index with abrupt peripheral decline. A decline in the lens nuclear refractive index with age has also been reported,[22,23] suggesting that the mechanism for the lens paradox may be twofold. The refractive contribution of GRIN and thus overall lens power has been estimated to decrease by 0.30 to 0.41 diopter (D)/year in isolated lenses,[23,24,29] but these values correspond to lenses in a state of maximal accommodation, which not only is uncertain but also varies with age.

We previously presented a platform that utilizes optical modeling to translate MRI-obtained measurements of lens geometry and GRIN to in vivo lens power.[30] Lens powers of seven healthy subjects with varying degrees of ametropia (–5.25 to 0.75 D) were measured with high fidelity, but our work was limited to young subjects (22 to 34 years) and did not explore the adaptability of the model to changes that are known to occur with aging of the lens.[4,5,22–28] The present work therefore aimed to extend the application of our platform to a larger cohort spanning a wider age range. In this study, we adapted our model for older lenses by characterizing their flatter GRIN profiles with customized power law expressions,[19,20,31,32] and we demonstrated that, by introducing an age-dependent factor into the existing transverse relaxation time (T_2) to refractive index (n) calibration,[24] our model was able to reproduce the clinically observed lens paradox. This optimized modeling approach highlights the need to gain further insight into how age-dependent changes to the GRIN at the molecular and cellular level manifest as changes to optical properties at the whole tissue level.

Methods

Subjects

We recruited 57 healthy subjects, evenly divided across three age groups: young (18–40 years), middle-aged (41–60 years), and older (>60 years) (Table 1). All subjects had best-corrected visual acuities (BCVA) of 6/12 or better, were free of visually significant ocular diseases (other than mild cataract), and had no previous intraocular surgery. All subjects completed a standard questionnaire to exclude those with an existing or previous diagnosis of diabetes mellitus and/or pre-diabetes and contraindications for undergoing MRI. Non-cycloplegic subjective refraction and BCVA were measured (AT20P Acuity Tester; Medmont, Nunawading, VIC, Australia). Maximum plus and binocular balance to ±0.25 D were administered. Ocular biometry was obtained with the Lenstar (Haag-Streit, Köniz, Switzerland). Ocular health examination under pupil dilation (1.0% tropicamide eye drops) was performed. Exclusion criteria included a mean sphere subjective refraction outside ±6 D and intraocular pressure >21 mm Hg. Right eyes were used unless the eye did not meet the criteria. All procedures were approved by the University of Auckland Human Subjects Ethics Committee and complied with the tenets of the Declaration of Helsinki. Written informed consent was obtained from all subjects.

Magnetic Resonance Imaging

All subjects underwent an MRI scan using a 3T clinical scanner (MAGNETOM Skyra; Siemens, Munich, Germany) located in the Centre for Advanced MRI at the University of Auckland. Procedures used in this study were similar to those reported previously.[30] Subjects laid supine on a table with their heads stabilized by foam pads. A 32-channel head receiver coil (Siemens) with viewing holes for both eyes was clamped in place. A mirror tilted 45° was attached to the coil, through which subjects viewed a customized target that consisted of a fixation crosshair combined with pictures that randomly changed every 5 seconds,[33] reflected from a screen display. This set-up gave a resultant viewing distance of about 2.1 meters. Our MRI protocol began with a set of localizer scans to center the lens within the field of view, followed by a high-resolution structural and then T_2 mapping scan. Subjects were instructed to avoid head movement and to maintain fixation on the target during data

acquisition. All sequences were performed with subjects' uncorrected vision. As such, they were informed that the target may appear blurry throughout the scan, but that it was more important to keep their eyes still rather than to focus on making the target clear. Time was given for subjects to rest their eyes between sequences. Total scan time lasted between 10 and 15 minutes. The image slice with the thickest lens visible was chosen for extracting lens geometry and T_2 maps. All raw MR images were postprocessed with custom-written routines in MATLAB (MathWorks, Natick, MA).

A turbo spin-echo (TSE) sequence (field of view [FoV] = 179 mm; matrix size = 448 × 448; slice thickness = 3 mm; echo time [T_E] = 116 ms; repetition time [T_R] = 2000 ms; parallel imaging acceleration factor = 2; total imaging time = 2.5 minutes) was used to obtain lens geometry. Measurements of lens anterior and posterior radii of curvature and axial thickness were extracted using established methods.[30] T_2 mapping was performed using a multiple spin-echo (MSE) sequence (FoV = 162.2 mm; matrix size = 768 × 768; slice thickness = 3 mm; T_R = 1600 seconds; parallel imaging acceleration factor = 2; total imaging time = 4.5 minutes). Ten echoes were acquired with the first T_E at 11.7 ms and with an echo spacing of 11.7 ms. Pixel-wise T_2 values were calculated using Equation 1:

$$\mathrm{S} = \mathrm{S}_0 e^{-\frac{TE}{T2}};\ S(TE) > \sigma \tag{1}$$

where S is the signal intensity at a given time, S_0 is the initial signal intensity, and σ is the noise threshold quantified from the image background.[34] Signal intensities at any T_E values below the noise threshold were discarded.[30] Each lens T_2 map was converted into a GRIN map using a calibration (Equation 2) previously derived from human donor lens homogenates by Jones et al.[24]:

$$n = 1.3554 + 1.549 \times 10^{-3}\left(\frac{1}{\mathrm{T2}}\right) - 6.34 \times 10^{-6}\left(\frac{1}{\mathrm{T2}}\right)^2 \tag{2}$$

where n is the refractive index and T_2 values are in seconds.

Isoindical contour plots were generated from each GRIN map. Points of intersections between anterior and posterior isoindical surfaces were connected with a second-order polynomial that was used to divide the lens into anterior and posterior hemispheres (Fig. 1). A GRIN profile was independently fitted in each hemisphere along the lens optical axis[30–32]:

$$\mathrm{n(r)} = \mathrm{n_{max}} + \delta_\mathrm{n} \mathrm{r^p} \tag{3}$$

where r is the radial distance from the lens surface, n_{max} is the lens central peak refractive index, δ_n is the refractive index variation between the lens center and periphery (such that it is negative when the peripheral index is lower), and exponent p characterizes the slope of the profile.

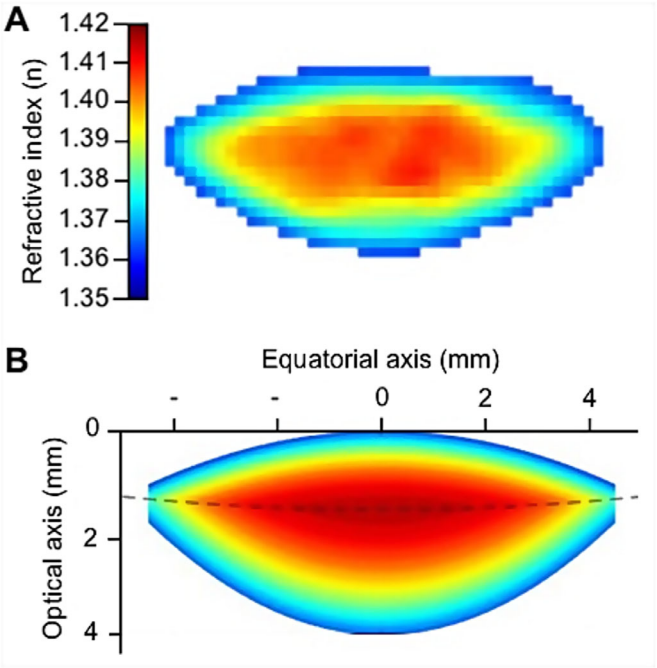

Figure 1. Postprocessing of lens GRIN map. (**A**) T_2 values were converted to refractive index values (n) to produce a two-dimensional GRIN map. (**B**) The raw GRIN map is fitted into a customized Zemax model to generate a smooth GRIN map based on isoindical contours. The points of intersections between anterior and posterior isoindical surfaces are connected to separate the two hemispheres.[31,32]

Zemax Modeling

Individual eye models were built using Zemax optical modeling software (Zemax, Kirkland, WA). Each model comprised six optical surfaces aligned along the keratometric axis: the cornea (anterior and posterior), lens (anterior, central, and posterior), and retina. The relative spacings of surfaces (i.e., central corneal thickness, anterior and vitreous chamber depths) were determined by the Lenstar, and the lens central interface was taken as the boundary between the lens hemispheres. The cornea was modeled as a rotationally symmetric conicoid with a refractive index of 1.376.[35] Both anterior and posterior corneal surfaces were assumed to have identical radii of curvature, taken as the average value of the flattest and steepest meridians in the central 3-mm zone measured with the Lenstar. Aqueous and vitreous humors had refractive indices of 1.336.[35] The lens was modeled as rotationally symmetric in both its external geometry

and GRIN distribution. The retina was modeled as a spherical surface.

Lens powers and ocular refractive errors were computed for monochromatic light ($\lambda = 587$ nm) through a 4-mm entrance pupil diameter. For lens power, the corneal surfaces were first removed so entrance rays were incident on the anterior lens. The lens was kept surrounded in the ocular humors (i.e., under in vivo conditions). The vitreous chamber depth was then set as a free variable and optimized to form the sharpest image on the retina. This represented the focal length of the lens which was converted into dioptric power. For ocular refractive errors, a surface simulating a spectacle lens was placed 14 mm in front of the cornea (the same back vertex distance at which subjective refraction was performed), and its radius of curvature was optimized to form the sharpest image on the retina. This was then converted into dioptric power and recorded as the ocular refractive error.

Calculation of an Age-Dependent Correction of the T_2-n Calibration

To optimize our model, an empirical age-dependent correction factor for the T_2-n calibration (Equation 2)[24] was determined using the concept of machine learning, as follows: First, 57 sets of acquired lens GRIN data were divided into a training set (approximately 75%, $n = 42$) and a testing set ($n = 15$). Within our training set, any difference between our model-calculated ocular refractive error and subjective refraction was eliminated for each eye model by adjusting the radius of curvature of the spectacle surface to match the mean sphere subjective refraction. The peak refractive index parameter (n_{max}) was then optimized to form the sharpest image on the retina. Optimal n_{max} values for each eye model were recorded and fitted against a product of their corresponding T_2 values and subject ages to derive the age-dependent correction factor for n. The resulting equation for the T_2-n calibration returned by the training set was

$$n_{max} = 1.4264 + 5.1 \times 10^{-3}(T_2 \times \text{age})^2 - 0.027 \times (T_2 \times \text{age}) \quad (4)$$

where n_{max} is the lens central peak refractive index, T_2 values are in seconds, and age is subject age in years.

The modified T_2-n calibration (Equation 4) was used to update n_{max} values of lens GRIN profiles in the testing set. The other GRIN profile parameters of refractive index variation (δ_n) and slope profile (exponent p) were left unaltered. Eye models in the testing set were then reconstructed with the newly derived n_{max} values, after which model-calculated ocular refractive errors displayed better agreement with subjective refractions. All GRINs in the training set were subsequently updated using Equation 4 and eye models reconstructed. Ocular refractive errors and lens powers were also recalculated for all eye models ($n = 57$). All training and testing tasks were performed using MATLAB.

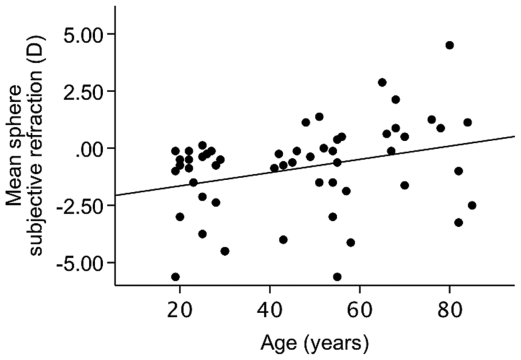

Figure 2. Age dependence of mean sphere subjective refraction. The equation for the regression line is given in Table 2.

Statistical Analysis

Analyses were performed using SPSS Statistics 25 (IBM, Armonk, NY) with a 5% significance level for all tests. Results are reported as mean ± SD. Linear regressions of parameters using age in years as the independent variable were calculated to determine age dependence.

Results

Not all parameters could be extracted from 57 subjects due to the poor MRI image quality obtained from one individual; hence, this individual was excluded from further analysis and only the results of 56 subjects were used to build the Zemax models. The age-dependent changes in subjective refraction, ocular biometry, and lens GRIN are first described, followed by their implementation into our modeling platform.

Age-Dependent Changes in Refractive Error, Ocular Biometry, and Lens GRIN

Refractive Error

There was a significant (0.029 D/year; $P = 0.021$) shift in subjective refraction toward hyperopia with age (Fig. 2). Although subjective refractions were not performed under cycloplegia and thus could be biased, our findings are in broad agreement with large population-based studies. The Blue Mountain[8,10]

Table 2. Age Dependence of Refractive Error and In Vivo Ocular Biometry

	Regression Equation	R^2	P
Mean sphere subjective refraction (D)*	−2.228 + 0.029 × age	0.095	0.021
Corneal central thickness (mm)	0.547 – 0.001 × age	0.004	0.648
Corneal curvature (mm)	7.975 – 0.003 × age	0.048	0.104
Axial length (mm)			
Uncorrected*	24.681 – 0.012 × age	0.070	0.028
After correction	24.012 – 0.004 × age	0.012	0.420
Lens thickness (mm)			
MRI*	3.237 + 0.018 × age	0.571	<0.001
Lenstar*	3.237 + 0.018 × age	0.643	<0.001
Lens radius of curvature (mm)			
Anterior*	13.430 – 0.072 × age	0.525	<0.001
Posterior*	−5.481 + 0.013 × age	0.199	<0.001
Anterior chamber depth (mm)*	3.403 – 0.011 × age	0.482	<0.001

*The results of the regression analysis were statistically significant.

and Beaver Dam Eye[6,7,12] studies, for example, have reported hyperopic shifts ranging from 0.12 to 0.29 D over a 5-year period.

Ocular Biometry

Corneal central thickness and corneal curvature showed no age dependence (Table 2). A decrease in axial length with age of some 0.012 mm/year was initially observed; however, after accounting for differences in refractive error among the subject populations with a correction factor of 0.30 mm/D[17], no significant age changes were found (Fig. 3A). Lens thickness measured by both the Lenstar and MRI increased 0.018 mm/year ($P < 0.001$) (Fig. 3B). Anterior and posterior lens radius of curvature steepened by 0.071 mm/year ($P < 0.001$) and 0.012 mm/year ($P = 0.001$), respectively (Fig. 3C). This was associated with a decrease of 0.011 mm/year ($P < 0.001$) in anterior chamber depth (Fig. 3D). In summary, our subject cohort exhibited age-dependent lens changes that were in good agreement with in vivo MRI[25,27,28] and Scheimpflug imaging[4,5] studies and confirmed that the major changes in ocular biometry were all associated with the crystalline lens.

Lens GRIN

As described in the methods (Fig. 1), T_2 values were initially converted into refractive index values (n) using a published calibration (Equation 2).[24] The resultant GRIN maps were subjected to contour smoothing and fitted as anterior and posterior profiles (Equation 3). From these maps, lens central peak index (n_{max}), refractive index variation (δ_n), and slope profile (p) values were extracted for each lens across our cohort of subjects. For all lenses across all ages, n along the optical axis was always highest in the central region and declined going toward the periphery, but GRIN profile shapes differed between age groups (Fig. 4A). Anterior p increased significantly (0.014/year; $P = 0.001$), indicating a sharper rate of decline in the refractive index from center to periphery with age (Fig. 4B). Posterior p showed no age change. The n_{max} values displayed a small but significant reduction with age (0.0000813/year; $P = 0.011$; Fig. 4C). δ_n showed no age dependence anteriorly but decreased in the posterior lens (0.000126/year; $P = 0.002$). Both observed trends of an increasing plateau[22–28] and reduction in refractive index variation[22,23] in our study cohort have previously been reported.

Zemax Modeling of Lens Power and Ocular Refractive Error

Age-Dependent Changes in Lens Power

The observed age-dependent changes in lens geometry in conjunction with those of GRIN would be expected to alter the overall power of the lens. Although we do not have true measures of in vivo lens powers against which to validate our calculations, assuming the hyperopic shift in subjective refraction of 0.029 D/year is due entirely to a concomitant loss of lens power from the lens paradox, we could consider this to be the target trend that our lens power calculations should approximate. However, our Zemax model calculations of lens power did not mirror our clinical observation, instead showing an increasing trend of 0.055 D/year (Fig. 5A).

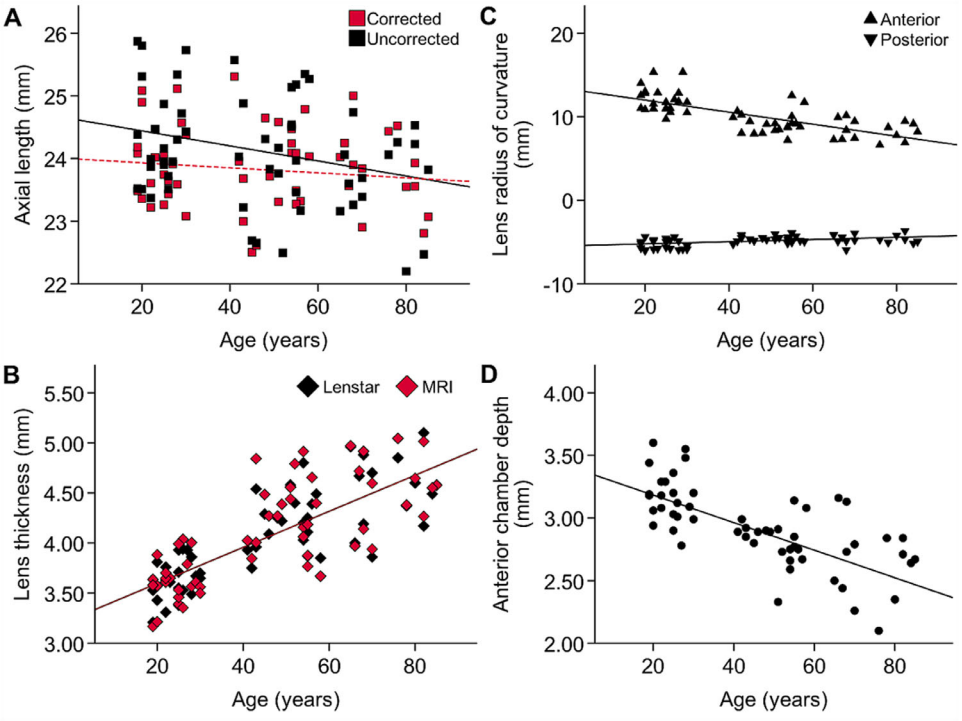

Figure 3. Age dependence of in vivo ocular biometry. (**A**) Axial length measured by the Lenstar before (*black*) and after (*red*) correction for refractive error. Axial lengths lose their age dependence after correction (*red dashed line*). (**B**) Central lens thickness measured by the Lenstar (*black*) and MRI (*red*). (**C**) Lens anterior (▲) and posterior (▼) surface radii of curvature measured by MRI. (**D**) Anterior chamber depth measured by the Lenstar. Significant age trends are indicated by *solid lines*, and the equations for the regression lines are given in Table 2.

Model Validation Against Refractive Error

The accuracy of our calculated lens powers was further assessed by comparing model-computed ocular refractive errors against subjective refractions. A Bland–Altman plot (Fig. 5B) shows that differences between the two measures were mostly between ±3 D. Simplifications of some components in our eye model—such as representing both corneal surfaces with just a single radius of curvature—would certainly contribute to these differences; such simplifications tend to overestimate corneal power by approximately 1.2 D on average in normal corneas.[36] A significant correlation between ocular refraction differences and subject age ($r = 0.570$; $P < 0.001$) (Fig. 5C) suggests that perhaps accommodation is another source of error due to the closer viewing distance of the MRI scan, but this would only account for a difference of 0.50 D.

The similar degrees of age dependency between ocular refraction differences (0.049 D/year) and lens power (0.055 D/year) indicate that the calculation inaccuracy was present regardless of whether or not all other optical elements of the eye were removed, suggesting that the main source of error is inherent to construction of the lens model. The two main determinants of lens power are its geometry and GRIN. We have previously shown that our MRI techniques measure lens geometry comparably to the gold standard of optical biometry (Lenstar),[30] so we can assume that any calculation inaccuracies likely stem from modeling of the GRIN. Because the GRIN profile shape has the potential of significantly influencing lens (and hence eye) power,[19,32] we used power functions in this study to minimize calculation inaccuracies arising from poor GRIN fittings in older lenses. With the lens refractive index left as the only remaining parameter, we proposed modifying peak indices by including an age factor into the T_2-n calibration of Jones et al.[24]

Model Correction with Age Factor

Peak refractive indices (n_{max}) derived by our modified calibration (Equation 4) decreased with age at a more prominent rate of 0.00038/year ($P < 0.001$) compared to that previously calculated from the published calibration (0.0000813/year). From a physiological and biochemical point of view, a decline in the lens peak index of this magnitude in the absence of a reciprocating decline in protein concentration (represented by T_2 measurements) is perfectly plausible. Figure 6 demonstrates the difference between

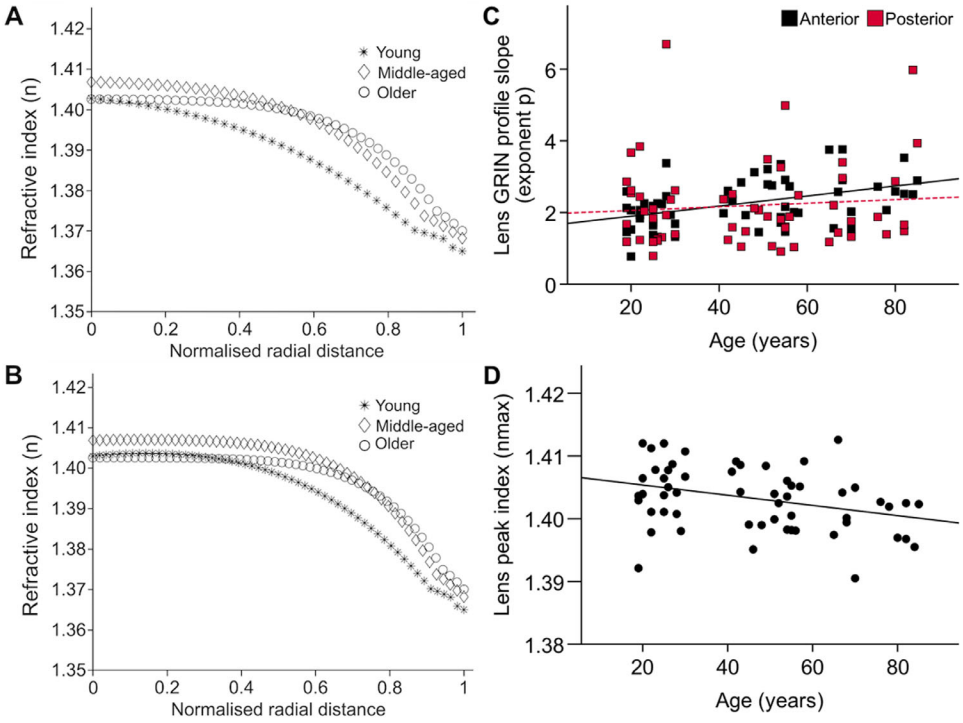

Figure 4. Age-dependent changes in the GRIN profile. Representative normalized (**A**) anterior lens and (**B**) posterior lens GRIN profiles modeled in young (30 years, ✳), middle-aged (41 years, ◇), and older (76 years, ○) subjects. Raw data from a representative lens from each group were used to generate these models. (**C**) Lens anterior (*black*) and posterior (*red*) GRIN profile slopes (exponent *p*) plotted against age. Posterior lens *p* shows no significant age dependence (*dashed red line*). (**D**) The lens peak refractive index (n_{max}) plotted against age. Significant age trends are indicated by *solid lines*.

Table 3. Comparison of Model-Calculated Outputs of Ocular Refraction and Lens Power Before and After Modification of the T_2-*n* Calibration

	Regression Equation	R^2	*P*
Difference in ocular refraction (D)			
Original*	−3.073 + 0.049 × age	0.325	<0.001
Modified	−0.162 − 0.007 × age	0.014	0.388
Lens power (D)			
Original*	17.364 + 0.055 × age	0.210	<0.001
Modified*	22.353 − 0.041 × age	0.134	0.005

*The results of the regression analysis were statistically significant.

lens GRIN profiles derived from the original[24] and our revised calibration.

Using n_{max} values derived by our revised calibration remarkably improved the validity of our model. The comparison of model outputs from the original and modified calibration is shown in Figure 7 and summarized in Table 3. Lens power calculations were more accurate; the mean calculated lens power of 20.46 ± 2.33 D matches reasonably well to the classic value of an unaccommodated lens,[35] and our lens power trend displayed a decreasing slope of similar magnitude as the clinical lens paradox (Fig. 7A). Differences in ocular refractions were reduced to mostly ±2.25 D (Fig. 7B), a magnitude that can be fully accounted for by test–retest variability (~6 ms) in central lens T_2 measurements alone.[30] Furthermore, for half of our cohort, it was reduced to within ±0.75 D, the variability of a subjective refraction measurement.[37] As expected, ocular refraction differences lost their age dependence (Fig. 7C) as a consequence of accounting for aging in the T_2-*n* calibration. Overall, modifying the T_2-*n* calibration made our model much

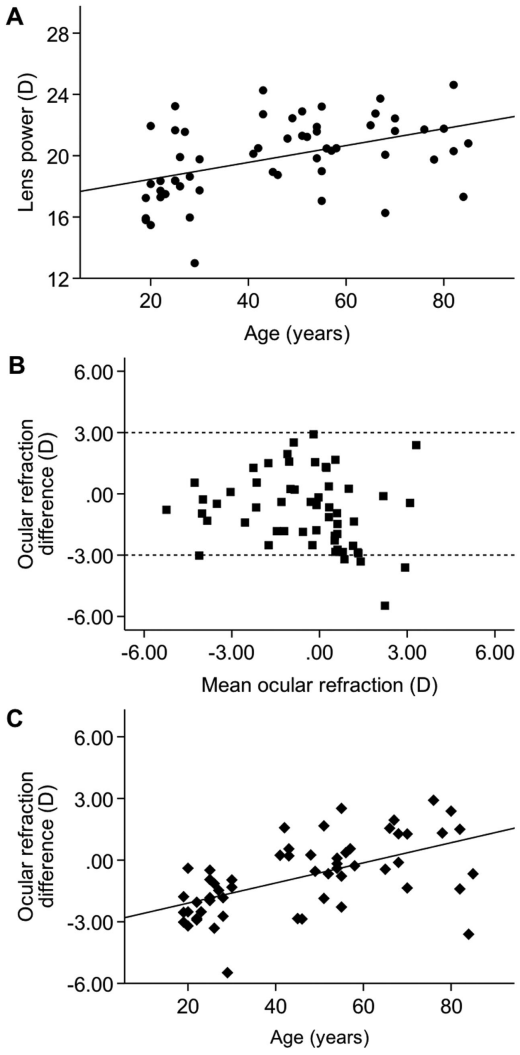

Figure 5. Assessment of the validity of our model-computed lens powers and ocular refractive errors. (**A**) Lens power plotted against age. (**B**) Bland–Altman plot showing ocular refraction differences between subjective refractions and model-calculated refractive errors lie mostly within ±3 D (*dashed lines*). (**C**) Ocular refraction difference plotted against age. Age dependence is similar to lens power, shown in **A**. Significant age trends are indicated by *solid lines*. The equations for the regression lines are given in Table 3.

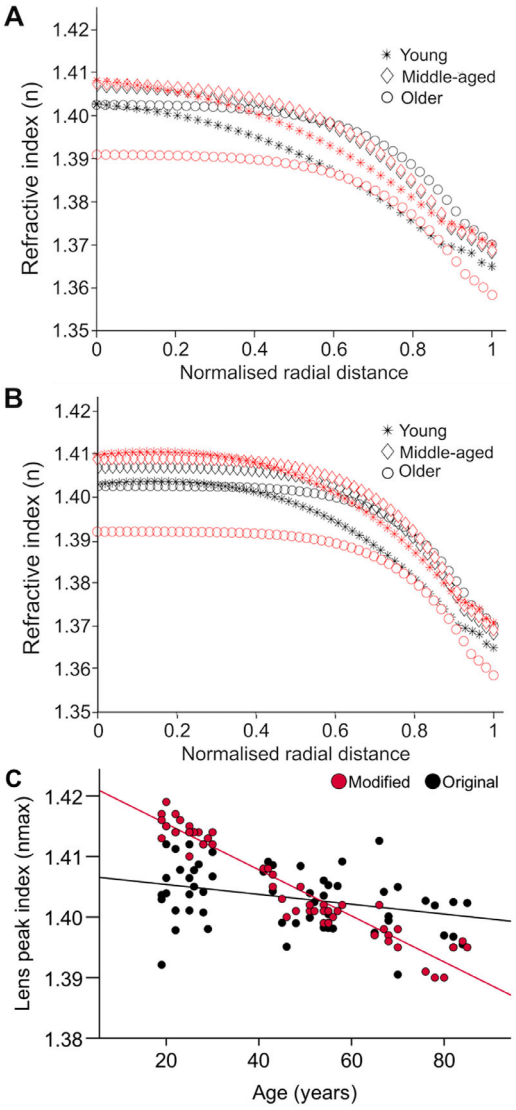

Figure 6. Comparison of lens GRIN profiles with (*red*) and without (*black*) our inclusion of an age-dependent factor in the T_2-n calibration. Representative normalized (**A**) anterior lens and (**B**) posterior lens GRIN profiles modeled in young (30 years, ✳), middle-aged (41 years, ◇), and older (76 years, ○) subjects. Raw data from a representative lens from each group were used to generate these models. (**C**) The lens peak refractive index (n_{max}) plotted against age. The rate of decline in n_{max} calculated using our modified T_2-n calibration is steeper than that calculated with the original calibration. Significant age trends are indicated by *solid lines*.

more robust, not just in its outputs but also in its representation of the underlying physiology of the crystalline lens.

Discussion

In this study, we applied our previously established optical modeling platform[30] and optimized it to more reliably calculate lens powers in vivo using experimental MRI data from subjects across a wide range of ages. Compared to the subject cohort upon which our platform was initially developed, the cohort of this study was considerably larger and older and exhibited flatter GRIN profiles at older ages. Therefore, for GRIN fitting in this study, we utilized a power function instead of the parabolic function used previously on younger lenses. In spite of this, our platform was unable to reproduce the expected lens power trend that we approximated as the age-dependent change in subjective refraction (i.e., the lens paradox) (Fig. 2). We therefore further optimized the model by modifying lens refractive indices by determining and implementing an

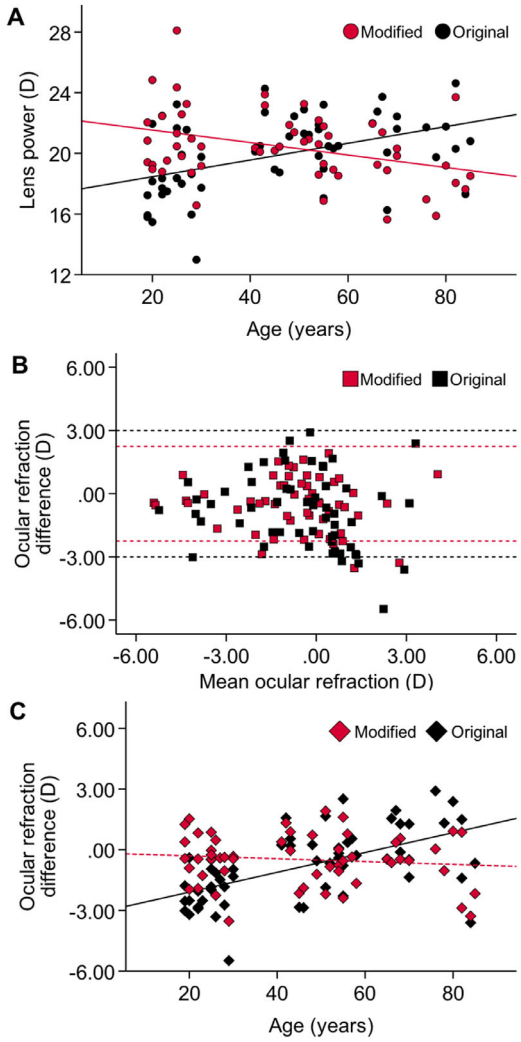

Figure 7. Comparison of the validity of our model-computed lens powers and ocular refractive errors, with (*red*) and without (*black*) our modification of the T_2-*n* calibration. (**A**) Lens powers before and after age correction, plotted against age. (**B**) Bland–Altman plot showing that ocular refraction differences have been reduced from mostly within ±3 D before (*black dashed lines*) to mostly within ±2.25 D after (*red dashed line*) age correction. (**C**) Ocular refraction differences before and after age correction, plotted against age. Ocular refraction differences lose their age dependence after age correction (*red dashed line*). Significant age trends are indicated by *solid lines*. The equations for the regression lines are given in Table 3.

age-dependent factor in the existing T_2-*n* calibration.[24] Using our modified calibration, the rate of decline in the lens central peak index with age was about two orders of magnitude greater than that determined by the original calibration (Fig. 6B). This closely agrees with the rate of nuclear index decline in human donor lenses in vitro (0.00034/year) reported using MRI by Moffat et al.[22,23] and that measured with a novel x-ray Talbot interferometry technique (0.0001/year).[38] Our model outputs were also notably improved; lens powers not only displayed the appropriate decreasing trend with age (Fig. 7A) but also occurred at a rate comparable to that of our cohort's hyperopic shift. These findings suggest that a notable reduction in the lens peak index and development of a central plateau in lens GRIN are both important factors for the decrease in GRIN refractive contribution to override the increase in geometric refractive contribution and, ultimately, drive the lens paradox.

The mutual dependency on lens protein concentration forms the basis of the conversion of T_2 measurements to refractive index,[22–28] but the relationship between protein and the refractive index is more complex than presumed by the original T_2-*n* calibration. Recent experiments have shown that the refractive index, although predominantly determined by amino acid composition, can differ under conditions of different pH levels or temperature and for folded or unfolded proteins.[39,40] At the same time, it is well established that proteins in the lens undergo multiple post-translational modifications with aging[41] that lead to alterations in conformation and likely molecular contribution toward the refractive index. Consequently, T_2, which correlates to protein concentration, may not necessarily reflect these age-related changes in protein structure and function. The same T_2 obtained from a young and older lens may therefore represent identical protein concentrations but differ in the refractive index. Because lens homogenates effectively average the refractive contribution of all lens proteins toward the GRIN, molecular changes that occur with age would not have been taken into account in the original calibration.[24] The inclusion of an age factor in the existing lens T_2-*n* calibration is thus not only justified but arguably essential.

Two possible explanations for a decline in the lens peak index have been raised[22,23]: (1) a decline in lens protein content, which has been previously reported,[42] or (2) aggregate formation due to a lifelong accumulation of major changes in lens crystallins at the molecular level.[43] In aggregate form, proteins cannot bind as much water because of a smaller net exposed surface area, thus becoming less soluble and losing some of their refractive contribution. At first glance, the small reduction in the lens peak index that we observed across the range of subject ages with the original T_2-*n* calibration might imply a decrease in central lens protein concentration (represented by T_2 measurements) and by extension a loss in protein content in that region. The need for an age-correction factor in the T_2-*n* calibration brought to attention by our modeling results, however, suggests the latter is the primary mechanism—the amount of protein in the lens undergoes little change throughout life but its refractive

contribution and resultant refractive indices lessens as aggregates form. These major changes in protein conformation are reflected in the steady increase in proportion of free water within the lens with age.[44–46] It has been estimated that the ratio of free to bound water in the lens is 1:1 at 20 years of age and progresses to 2:1 by between 70 and 80 years of age.[46] Finally, the plausibility of a loss of protein content should be carefully considered given the inability of lens cells to break down and/or remove proteins. Of course, a third possibility for a decline in nuclear protein concentration and thus the refractive index is an increase in total water content in the nucleus. However, there is currently no clear agreement about what happens to water content in the nucleus of aged lenses, with some studies reporting an increase[42] or a decrease,[47] and others finding no change.[48] Further investigation is necessary to determine what effect lens local water state and content may have on the refractive index.

Although the age-dependent changes in lens protein–water interactions are taken into account with our modification of the original T_2-n calibration[24] and result in the ability of our model to accurately calculate in vivo lens powers, there remains theoretical issues to consider. The first is that we have derived our age-correction factor based on the agreement between measures of ocular refraction rather than direct measurements of lens GRIN and/or protein concentration. Proper modification of the calibration would require correlating lens T_2 profiles with independently acquired lens GRIN profiles. Our lab has recently developed a fully automated laser ray tracing system that has been shown to reliably measure the GRIN profiles of in vitro bovine lenses.[49] Modifying this system to measure human donor lens GRINs will help identify how we can more appropriately modify the T_2-n calibration and is the subject of future work. Another limitation is our over-simplification of characterizing the aging process with a single factor. Doing so assumes that all lens proteins age uniformly, but this is presumably not the case; increasing age is more strongly associated with the development of cataract in the lens nucleus than elsewhere (e.g., cortical cataract).[50] It should also be noted that the central plateau of the constant refractive index in the lens GRIN reaches a maximum width at around 60 years of age[26]; therefore, beyond this point, a decline in the nuclear index will have a lesser effect on overall lens power. This suggests that refractive index changes also occur in proteins located in the lens cortex, as this would be required for the refractive contribution of the GRIN to continually offset the contribution from an increased rounding in lens curvature. Future calibration revisions could benefit from having multiple factors to describe the different effects aging has on the various distributions and types of proteins in the different regions of the lens.

In conclusion, we have modified an almost two-decade-old calibration and have demonstrated our platform to more reliably calculate in vivo lens powers as a result. This study has highlighted that more information regarding the impact of physiological changes of the lens on its refractive properties is required for a better understanding of age-dependent changes in lens optics such as presbyopia and cataract and ultimately has implications on how to prevent the decline in vision quality associated with these conditions.

Acknowledgments

The authors thank the volunteer subjects for their time. We also thank the radiographers at CAMRI for their assistance with performing MRI scans; Safal Khanal, PhD, for the opportunity to use his MRI fixation target; and Robin Laven for automating our optical modeling platform.

Supported by a Grant from the National Institutes of Health (EY026911). During the period of this research study and preparation for publication, Author A.L. Lie received doctoral scholarship support from the HOPE Selwyn Foundation and the New Zealand Association of Optometrists.

Disclosure: **A.L. Lie,** None; **X. Pan,** None; **T.W. White,** None; **P.J. Donaldson,** None; **E. Vaghefi,** None

References

1. Brown N. The change in lens curvature with age. *Exp Eye Res*. 1974;19:175–183.
2. Brown NP, Koretz JF, Bron AJ. The development and maintenance of emmetropia. *Eye*. 1999;13:83–92.
3. Bron A, Vrensen G, Koretz J, Maraini G, Harding J. The ageing lens. *Ophthalmologica*. 2000;214:86–104.
4. Dubbelman M, Van der Heijde GL. The shape of the aging human lens: curvature, equivalent refractive index and the lens paradox. *Vision Res*. 2001;41:1867–1877.
5. Atchison DA, Markwell EL, Kasthurirangan S, Pope JM, Smith G, Swann PG. Age-related

changes in optical and biometric characteristics of emmetropic eyes. *J Vis*. 2008;8:1–20.
6. Lee KE, Klein BEK, Klein R. Changes in refractive error over a 5-year interval in the Beaver Dam Eye Study. *Invest Ophthalmol Vis Sci*. 1999;40:1645–1649.
7. Lee KE, Klein BEK, Klein R, Wong TY. Changes in refraction over 10 years in an adult population: the Beaver Dam Eye Study. *Invest Ophthalmol Vis Sci*. 2002;43:2566–2571.
8. Guzowski M, Wang JJ, Rochtchina E, Rose KA, Mitchell P. Five-year refractive changes in an older population: the Blue Mountains Eye Study. *Ophthalmology*. 2003;110:1364–1370.
9. Gudmundsdottir E, Arnarsson A, Jonasson F. Five-year refractive changes in an adult population: Reykjavik Eye Study. *Ophthalmology*. 2005;112:672–677.
10. Fotedar R, Mitchell P, Burlutsky G, Wang JJ. Relationship of 10-year change in refraction to nuclear cataract and axial length. *Ophthalmology*. 2008;115:1273–1278.
11. Goldblum D, Burgger A, Haselhoff A, Schmickler S. Longitudinal change of refraction over at least 5 years in 15,000 patients. *Graefes Arch Clin Exp Ophthalmol*. 2013;251:1431–1436.
12. Bomotti S, Lau B, Klein BEK, et al. Refraction and change in refraction over a 20-year period in the Beaver Dam Eye Study. *Invest Ophthalmol Vis Sci*. 2018;59:4518–4524.
13. Koretz JF, Kaufman PL, Neider MW, Goeckner PA. Accommodation and presbyopia in the human eye—aging of the anterior segment. *Vision Res*. 1989;29:1685–1692.
14. Ooi CS, Grosvenor T. Mechanisms of emmetropization in the aging eye. *Optom Vis Sci*. 1995;72:60–66.
15. Eysteinsson T, Jonasson F, Sasaki H, et al. Central corneal thickness, radius of the corneal curvature and intraocular pressure in normal subjects using non-contact techniques: Reykjavik Eye Study. *Acta Ophthalmol Scand*. 2002;80:11–15.
16. Dubbelman M, Sicam VADP, Van der Heijde GL. The shape of the anterior and posterior surface of the aging human cornea. *Vision Res*. 2006;46:993–1001.
17. Koretz JF, Cook CA. Aging of the optics of the human eye: lens refraction models and principal plane locations. *Optom Vis Sci*. 2001;78:396–404.
18. Diaz JA, Pizarro C, Arasa J. Single dispersive gradient-index profile for the aging human lens. *J Opt Soc Am A*. 2008;25:250–261.
19. Smith G, Pierscionek BK, Atchison DA. The optical modelling of the human lens. *Ophthalmic Physiol Opt*. 1991;11:359–369.
20. Smith G, Atchison DA, Pierscionek BK. Modeling the power of the aging human eye. *J Opt Soc Am A*. 1992;9:2111–2117.
21. Pierscionek BK, Chan DYC. Refractive index gradient of human lenses. *Optom Vis Sci*. 1989;66:822–829.
22. Moffat BA, Atchison DA, Pope JM. Explanation of the lens paradox. *Optom Vis Sci*. 2002;79:148–150.
23. Moffat BA, Atchison DA, Pope JM. Age-related changes in refractive index distribution and power of the human lens as measured by magnetic resonance micro-imaging in vitro. *Vision Res*. 2002;42:1683–1693.
24. Jones CE, Atchison DA, Meder R, Pope JM. Refractive index distribution and optical properties of the isolated human lens measured using magnetic resonance imaging (MRI). *Vision Res*. 2005;45:2352–2366.
25. Jones CE, Atchison DA, Pope JM. Changes in lens dimensions and refractive index with age and accommodation. *Optom Vis Sci*. 2007;84:990–995.
26. Augusteyn RC, Jones CE, Pope JM. Age-related development of a refractive index plateau in the human lens: evidence for a distinct nucleus. *Clin Exp Optom*. 2008;91:296–301.
27. Kasthurirangan S, Markwell EL, Atchison DA, Pope JM. In vivo study of changes in refractive index distribution in the human crystalline lens with age and accommodation. *Invest Ophthalmol Vis Sci*. 2008;49:2531–2540.
28. Adnan Pope JM, Sepehrband F, et al. Lens shape and refractive index distribution in type 1 diabetes. *Invest Ophthalmol Vis Sci*. 2015;56:4759–4766.
29. Borja D, Manns F, Ho A, et al. Optical power of the isolated human crystalline lens. *Invest Ophthalmol Vis Sci*. 2008;49:2541–2548.
30. Pan X, Lie AL, White TW, Donaldson PJ, Vaghefi E. Development of an in vivo magnetic resonance imaging and computer modelling platform to investigate the physiological optics of the crystalline lens. *Biomed Opt Express*. 2019;10:4462–4478.
31. Navarro R, Palos F, Gonzalez LM. Adaptive model of the gradient index of the human lens. I. Formulation and model of aging ex vivo lenses. *J Opt Soc Am A*. 2007;24:2175–2185.
32. Navarro R, Palos F, Gonzalez LM. Adaptive model of the gradient index of the human lens. II. Optics of the accommodating aging lens. *J Opt Soc Am A*. 2007;24:2911–2920.

33. Thaler L, Schütz AC, Goodale MA, Gegenfurtner KR. What is the best fixation target? The effect of target shape on the stability of fixational eye movements. *Vision Res*. 2013;76:31–42.
34. Dietrich O, Raya JG, Reeder SB, Reiser MF, Schoenberg SO. Measurement of signal-to-noise ratios in MR images: influence of multichannel coils, parallel imaging, and reconstruction filters. *J Magn Reson Imaging*. 2007;26:375–385.
35. Gullstrand A. Appendices II and IV. In: von Helmholtz H, ed., *Helmholtz's Handbuch der Physiologischen Optik*. Leipzig, Germany: Leopold Voss; 1909:301–358, 382–415.
36. Hernandez VM, Cabot F, Ruggeri M, et al. Calculation of crystalline lens power using a modification of the Bennett method. *Biomed Opt Express*. 2015;6:4501–4515.
37. Leinonen J, Laakkonen E, Laatikainen L. Repeatability (test-retest variability) of refractive error measurement in clinical settings. *Acta Ophthalmol Scand*. 2006;84:532–536.
38. Pierscionek B, Bahrami M, Hoshino M, Uesugi K, Regini J, Yagi N. The eye lens: age-related trends and individual variations in refractive index and shape parameters. *Oncotarget*. 2015;6:30532–30544.
39. Zhao H, Brown PH, Schuck P. On the distribution of protein refractive index increments. *Biophys J*. 2011;100:2309–2317.
40. Khago D, Bierma JC, Roskamp KW, Kozlyuk N, Martin RW. Protein refractive index increment is determined by conformation as well as composition. *J Phys Condens Matter*. 2018;30:435101–435109.
41. Hains PG, Truscott RJ. Post-translational modifications in the nuclear region of young, aged, and cataract human lenses. *J Proteome Res*. 2007;6:3935–3943.
42. Siebinga I, Vrensen GF, De Mul FF, Greve J. Age-related changes in local water and protein content of human eye lenses measured by Raman microspectroscopy. *Exp Eye Res*. 1991;53:233–239.
43. Bloemendal H, de Jong W, Jaenicke R, Lubsen NH, Slingsby C, Tardieu A. Ageing and vision: structure, stability and function of lens crystallins. *Prog Biophys Mol Biol*. 2004;86:407–485.
44. Lahm D, Lee K, Bettelheim FA. Age dependence of freezable and nonfreezable water content of normal human lenses. *Invest Ophthalmol Vis Sci*. 1985;26:1162–1165.
45. Bettelheim FA, Lizak MJ, Zigler JS. Relaxographic studies of aging normal human lenses. *Exp Eye Res*. 2002;75:695–702.
46. Heys KR, Friedrich MG, Truscott RJW. Free and bound water in normal and cataractous human lenses. *Invest Ophthalmol Vis Sci*. 2008;49:1991–1997.
47. Fisher RF, Pettet BE. Presbyopia and the water content of the human crystalline lens. *J Physiol*. 1973;234:443–447.
48. Heys KR, Cram SL, Truscott RJW. Massive increase in the stiffness of the human lens nucleus with age: the basis for presbyopia? *Mol Vis*. 2004;10:956–963.
49. Qiu C, Maceo Heilman B, Kaipio J, Donaldson P, Vaghefi E. Fully automated laser ray tracing system to measure changes in the crystalline lens GRIN profile. *Biomed Opt Express*. 2017;8:4947–4964.
50. Age-Related Eye Disease Study Research Group. Risk factors associated with age-related nuclear and cortical cataract: a case-control study in the Age-Related Eye Disease Study, AREDS Report No. 5. *Ophthalmology*. 2001;108:1400–1408.